

Improved sensorless backstepping controller using extended Kalman filter of a permanent magnet synchronous machine

Abderrahmen Kirad¹, Said Grouni¹, Youcef Soufi²

¹Department of Automation, Faculty of Hydrocarbons and Chemistry, Applied Automation Laboratory, University of M'Hamed, Bougara, Boumerdes, Algeria

²Department of Electrical Engineering, Faculty of Sciences and Technology, Labget Laboratory, University Larbi Tebessi, Tebessa, Algeria

Article Info

Article history:

Received Jul 28, 2021

Revised Dec 13, 2021

Accepted Feb 28, 2022

Keywords:

Extended Kalman filter

Field oriented control

Lyapunov approach

Nonlinear backstepping control

Permanent magnet synchronous motor

Sensorless control

ABSTRACT

This paper deals with an improved backstepping control strategy for sensorless control of a permanent magnet synchronous motor (PMSM) based on field-oriented control (FOC), using a backstepping controller to improve its performances. However, this control requires the precise knowledge of some machine's variables which could not be available. In electric drives control, sensors are generally used as the main devices for feedback information. Some practical constraints could affect the system performances, due to the lack of measurement material or maintenance difficulties caused by the dysfunction or faults of the used sensors such as: encoder or resolver sensors of speed-position. In this paper, a sensorless control is proposed based on a dynamic backstepping method and an extended Kalman filter (EKF) which uses the state space formulation with a set of mathematical equations to recursively estimate future observations and minimizes the mean square error of the estimated variables (rotor speed position and torque) to design controllers for nonlinear systems. The proposed control scheme achieves the asymptotically uniformed stability. The effectiveness of this method is illustrated by the stabilization and tracking numerical examples and the obtained simulation results show the effectiveness and the feasibility of the proposed controller using Lyapunov approach.

This is an open access article under the [CC BY-SA](https://creativecommons.org/licenses/by-sa/4.0/) license.



Corresponding Author:

Abderrahmen Kirad

Department of Automation, Faculty of Hydrocarbons and Chemistry, Applied Automation Laboratory

Université M'Hamed Bougara

Boumerdes, 35000 Algeria

Email: a.kirat@univ-boumerdes.dz

1. INTRODUCTION

Permanent magnet synchronous motor (PMSM) is widely used in industrial applications compared to other electric motors such as: induction motor (IM), direct current (DC) motor and switched reluctance motor (SRM) based on the required characteristics [1], [2]. Mainly, due to its compact design, high efficiency, high torque to inertia ratio, high dynamic response, excellent reliability, great robustness, power density, technological maturity, a gap for advancement in controller design, small volume, and reduced maintenance [3]–[5]. In other side, the non-linearity of the dynamic model of the PMSM produces a large specific control difficulty [6], [7]. Parameters, load torque variations also the coupling between the motor speed and the electrical quantities, such as the d-q axis currents, make this system obviously hard to control [3], [8], [9]. This motor can be controlled by the conventional proportional integral (PI) classical controller

[10], [11]. A large techniques and approaches of PMSM nonlinear control have been extremely studied, developed and proposed such as: input-output linearization control [12], robust control [13], sliding mode control [14]–[16], back-stepping control [17], [18], fuzzy logic control [19], direct torque control (DTC) [20], [21], and linear parameter varying (LPV) [22]. But the problem or difficulties facing the used approaches are: the proportional integral derivative (PID) controller cannot guarantee satisfactory performance such as: stability and control against disturbances. However, the problem of chattering of sliding mode controller (SMC) requires control that can switch at an infinite frequency. Thus, during the sliding regime, the discontinuities applied to the control can train to chattering phenomena, called reluctance or "chattering". These switchings deteriorate the control precision, can prove deterioration of mechanical parts of the systems and increase the the temperature in electrical systems (significant loss of energy). However, we must keep in mind that in fuzzy logic, it is impossible to predict the performance of a system due to its dependence on the well selection of the setting parameters. On the other hand, for the DTC control strategy, the oscillations of the various variables are sensitive, compared to the current-voltage measurement sensors, and limed by the controlled variables: the torque and stator flux. Recently, the back-stepping presents promisingly alternative methods for controlling nonlinear systems by combining the choice of the Lyapunov function with the control laws which allows the overall stability of the system [17], [23].

Since mechanic position and speed sensors (encoder, resolver or hall sensor) are usually too expensive, they increase the cost and complexity, decrease the stability of the system, impose hard maintenance, and are sensitive to noise. Thus, sensor-less control is becoming very attractive research and a big challenging task [18]. The state observer permits an accurate estimation of the speed and the position in the presence of system noise and parameters variations. The sensorless PMSM control has been exausted in the last decades. Trabelsi *et al.* [18] proposed the control of sensorless PMSM using sliding mode observer, Luenberger [23], back-electromotive force (back-EMF) [24], model reference adaptive system method (MRAS) has proved [25], or the artificial intelligence. Among those, the extended Kalman filter (EKF) is the most well-known and optimal one, especially in the presence of the process and measurement noise [26]–[30] which is well adapted to nonlinear systems and such applications. In this paper, an optimal PMSM field-oriented control strategy is proposed, using a backstepping controller and an EKF based on a recursive method to estimate the rotor speed position of the considered machine and to minimize the mean squared error.

The contribution in the present work focuses on the combination of the EKF with backstepping control in order to estimate the parameters or the measurement of the state machine due to the fort non linearity of system parametres and the faced difficulties in the sensors, based on backstepping approach for better tracking of the speed by introducing the estimation of both rotor speed-position and electromagnetic torque respective. The main advantage of introducing such controller is its skills to cope with some drawbacks of the PI controller. In practice, each variable requires two controller gains, which are continuously changed, due to some of imprecise phenomena in the system. In contrast of that, and as developed later, less control variables are used, which guaranties the stability of the system via the choice of only three positive gains. Furthermore, an EKF is used to estimate both the rotor speed and position, as can be seen in Figure 1. A sensor-less control is introduced to increase the robustness, to ensures better dynamic, high performances, and decreases the cost and complexity.

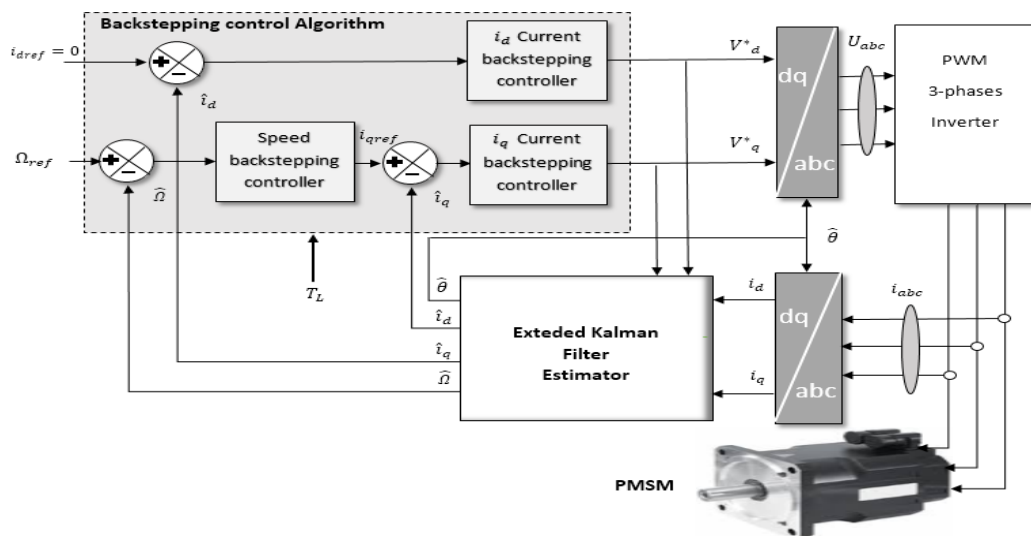


Figure 1. The proposed nonlinear sensorless controller of PMSM

To achieve the proposed approach, the rest of the paper is organized as; section 2, is reserved to the mathematical model presentation of the considered machine. The design of the backstepping controller is presented in section 3. Section 4, is dedicated to the design of the nonlinear sensor-less control using EKF. The simulation results demonstrate the effectiveness of the proposed control which are illustrated and commented in section 5, followed finally by a conclusion. As perspective, we plan to optimize the developed algorithms by the advanced approaches such as: particle swarm optimization (PSO), wolf gray, genetic algorithm (GA), neural network, and implement them experimentally with embedded control devices such as: (*STM32F407*) with its fourth-generation *M4* processor and Infineon type intelligent power module (IPM) for power part.

2. PMSM MATHMATICAL MODEL

The dynamic nonlinear model of PMSM in the (d-q) reference frame is given as [12], [15]:

$$\begin{cases} \frac{di_d}{dt} = -\frac{R_s}{L_d} i_d + \frac{L_q}{L_d} p i_q \Omega + \frac{1}{L_d} V_d \\ \frac{di_q}{dt} = -\frac{R_s}{L_q} i_q + \frac{L_d}{L_q} p i_d \Omega - \frac{p\Phi_f}{L_q} \Omega + \frac{1}{L_q} V_q \\ \frac{d\Omega}{dt} = \frac{3p\Phi_f}{2J} i_q + \frac{3P}{2J} (L_d - L_q) i_d i_q - \frac{f}{J} \Omega - \frac{1}{J} T_L \end{cases} \quad (1)$$

By choosing : $x = [i_d \ i_q \ \Omega]^T = [x_1 \ x_2 \ x_3]^T$ as a state vector and the load torque T_L as an external disturbance, $u = [V_d \ V_q]^T$ as control vector, Then we can write the state model of the machine in the form:

$$\begin{bmatrix} \dot{x}_1 \\ \dot{x}_2 \\ \dot{x}_3 \end{bmatrix} = \begin{bmatrix} -\frac{R_s}{L} & p x_3 & 0 \\ p x_3 & -\frac{R_s}{L} & -\frac{p\Phi_f}{L} \\ 0 & \frac{3p\Phi_f}{2J} & -\frac{f}{J} \end{bmatrix} \begin{bmatrix} x_1 \\ x_2 \\ x_3 \end{bmatrix} + \begin{bmatrix} \frac{1}{L} \\ 0 \\ 0 \end{bmatrix} \begin{bmatrix} V_d \\ V_q \end{bmatrix} + \begin{bmatrix} 0 \\ 0 \\ -\frac{1}{J} T_L \end{bmatrix}, y = \begin{bmatrix} x_1 \\ x_2 \\ x_3 \end{bmatrix} \quad (2)$$

The dynamic model of the nonlinear system is presented with the following representation (3):

$$\begin{cases} \frac{dx}{dt} = f(x) + g \cdot u + w \\ y = h(x) \end{cases}, \text{ with: } f(x) = Ax \text{ and } h(x) = Cx \quad (3)$$

3. BACKSTEPPING CONTROL DESIGN

The recursive back-stepping technique guarantees the asymptotic stability of the system in close loop, by choosing an adequate Lyapunov function for stabilizing error variables [16], [18], [23], [31]. Furthermore, the controller is very efficient for nonlinear systems. In fact, the PMSM dynamic model is highly nonlinear, and such control technique can be applied directly with no linearization. The vector control principle is generally introduced to assimilate the considered machine control to the DC motor. The i_d current is always forced to be zero [24] by the orientation of the all linkage flux in the d axis to obtain the maximum torque. The principal objective of the proposed back-stepping controller is to ensure the reference speed tracking of the PMSM drive in the presence of external disturbances changing (the torque load) [24]. The proposed robust controller is designed in two steps is being as: the first step concerns the speed controller design methodology and the second, incorporates an imbricate current controller, via an augmented Lyapunov function.

3.1. Speed control design methodology

The speed loop tracking error variable and its derivative is given respectively by (4) and (5)

$$e_{x_3} = x_{3_{ref}} - x_3 \quad (4)$$

$$\dot{e}_{x_3} = \dot{x}_{3_{ref}} - \dot{x}_3 \quad (5)$$

From (2) and (5), the speed error derivative becomes:

$$\dot{e}_{x_3} = \dot{x}_{3_{ref}} - \frac{3p\Phi_f}{2J} x_2 + \frac{f}{J} x_3 + \frac{1}{J} T_L \quad (6)$$

By choosing a positive candidate Lyapunov function:

$$V_1 = \frac{1}{2} e_{x_3}^2 \tag{7}$$

Its derivative is given by:

$$\dot{V}_1 = e_{x_3} \dot{e}_{x_3} = e_{x_3} \left(\dot{x}_{3ref} - \frac{3p\Phi_f}{2J} x_2 + \frac{f}{J} x_3 + \frac{1}{J} T_L \right) \tag{8}$$

The back-stepping design method considers the d-q axes currents x_1 and x_2 as virtual control elements and specify its desired behavior, which are called stabilizing function in the backstepping design terminology is being as:

$$\begin{cases} x_{1ref} = 0 \\ x_{2ref} = \frac{2}{3p\Phi_f} (fx_3 + T_L + J \cdot K_{x_3} \cdot e_{x_3}) \end{cases} \quad \text{With } K_{x_3} \text{ is a positive constant} \tag{9}$$

In order to guarantee the reference tracking and according to Lyapunov stability theory, the condition $\dot{V}_1 < 0$ must be verified. Substituting (9) in (8) the derivative of V_1 , one gets:

$$\dot{V}_1 = -K_{x_3} e_{x_3}^2, K_{x_3} > 0 \tag{10}$$

Therefore, the speed error approaches zero and global asymptotic stability is achieved.

3.2. Backstepping current controller

To ensure, the asymptotic stability of the system (1), a second step is added, allowing the d-q currents to match the set values. The following current errors are defined as:

$$\begin{cases} e_{x_1} = x_{1ref} - x_1 \\ e_{x_2} = x_{2ref} - x_2 \end{cases} \quad \text{with } x_{1ref} = 0 \tag{11}$$

Their dynamics can be written:

$$\dot{e}_{x_1} = \dot{x}_{1ref} - \dot{x}_1 = \frac{R_S}{L} x_1 - px_2x_3 - \frac{1}{L} V_d \tag{12}$$

$$\dot{e}_{x_2} = \dot{x}_{2ref} - \dot{x}_2 = \frac{2}{3p\Phi_f} (fx_3 + T_L + J \cdot K_{x_3} \cdot e_{x_3}) + \frac{R_S}{L} x_2 + px_1x_3 + \frac{p\Phi_f}{L} x_3 - \frac{1}{L} V_q \tag{13}$$

The stability of the studied system is analyzed based on Lyapunov function (14):

$$V_2 = \frac{1}{2} (e_{x_3}^2 + e_{x_1}^2 + e_{x_2}^2) \tag{14}$$

Based on (6), (12), and (13) the derivative of (14) is given by:

$$\dot{V}_2 = e_{x_3} \dot{e}_{x_3} + e_{x_1} \dot{e}_{x_1} + e_{x_2} \dot{e}_{x_2} \tag{15}$$

$$\begin{aligned} \dot{V}_2 = & -k_{x_3} e_{x_3}^2 - k_{x_1} e_{x_1}^2 - k_{x_2} e_{x_2}^2 + e_{x_1} \left[k_{x_1} e_{x_1} - \frac{V_d}{L} + \frac{R_S}{L} - x_3 x_2 \right] + \\ & e_{x_2} \left[k_{x_2} e_{x_2} \frac{2(k_{x_3}J-f)}{3p\Phi_f} \left(\frac{3p\Phi_f}{2J} e_{x_2} - k_{x_3} e_{x_3} \right) + \frac{3p\Phi_f}{2J} e_{x_3} - \frac{V_q}{L} + \frac{R_S}{L} x_2 + x_3 x_1 + x_3 \frac{\Phi_f}{L} \right] \end{aligned} \tag{16}$$

The expression (15) must be defined semi negative, and consequently the control laws are deduced as:

$$V_d = k_{x_1} L e_{x_1} + R_S x_1 - L x_3 x_2 \tag{17}$$

$$V_q = \frac{2(k_{x_3}J-f)}{3p\Phi_f} \left(\frac{3p\Phi_f}{2J} e_{x_2} - k_{x_3} e_{x_3} \right) + \frac{3p\Phi_f L}{2J} e_{x_3} + R_S x_2 + L x_3 x_1 + x_3 \Phi_f + k_{x_2} L e_{x_2} \tag{18}$$

With this choice, the derivatives of (14) become:

$$\dot{V}_2 = -k_\Omega e_\Omega - k_d e_d - k_q e_q < 0 \tag{19}$$

This means that the tracking errors will converge asymptotically to zero.

4. SPEED AND POSITION OBSERVER DESIGN USING EXTENDED KALMAN FILTER

In this section, the EKF observer is applied to estimate the PMSM rotor speed and position in order to achieve the feedback process control performed by the previous back-stepping control strategy.

4.1. Extended Kalman filter principle

The EKF is a mathematical tool working in iteration and numerical way, able to reconstruct the system states from other measurable physical variables [26]. This estimator is an optimal predictor-corrector which it minimizes the estimated error covariance when some presumed conditions are occurred [26]. For the speed and the position estimation of PMSM, where parameters variation and measurement noise are present, EKF is the ideal one [32], [33]. The Figure 2 illustrates the EKF principle. The EKF reposes on some hypothesis especially the noise. Effectively, it supposes that the noises which affect the model are Gaussian and white and are decorrelated from estimated states [32].

$$\begin{cases} x_k = f(x_{k-1}, u_{k-1}) + w_{k-1} \\ y_k = h(x_k) + v_k \end{cases} \tag{20}$$

Where, $x_k = [i_{d_k} \ i_{q_k} \ \Omega_{r_k} \ \theta_k \ T_{L_k}]^T$; The estimated vector; $y_k = [h_1 \ h_2]^T$ The system output; u_k : the control law; w_k : noise process; v_k : noise measurement are respectively stand for errors of the parameters and measurement; $f(x_{k-1}, u_{k-1}), h(x_k)$: nonlinear functions, where: $f(x_{k-1}, u_{k-1}) = x_{k-1} + \dot{x}_{k-1}T_s$; T_s is the sampling time and $h(x_k) = \begin{bmatrix} i_{d_k} \\ i_{q_k} \end{bmatrix}$. The noise covariance matrixes are defined is being as:

$$Q = cov(w) = cov(w, w^T) = E(w, w^T) \tag{21}$$

$$R = cov(v) = cov(v, v^T) = E(v, v^T) \tag{22}$$

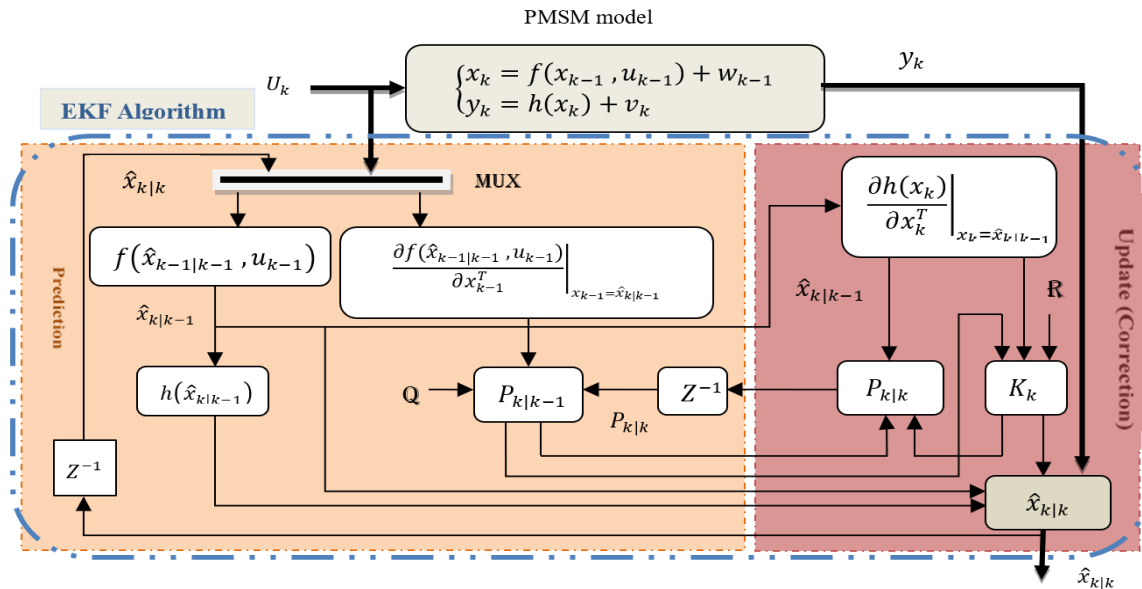


Figure 2. Simplified scheme of the EKF principle

The choice of the covariance matrices elements is the critical point in the design of EKF which is related to the performance and the convergences of the system. The two matrices Q and R depend on the training parameters, the sampling time of the amplitudes of the measurements, and some other secondary

factors. Also, the robustness of the EKF is linked to the chosen values of the sampling time, which is generally linked to the switching frequency and also linked to the capacity of the control board used. In practice, the sampling time is linked to the execution speed like the DSP board [34], [35]. The EKF estimation procedure is realized in two steps: prediction and correction (update).

4.1.1. Prediction time update

In this phase, a prediction of the state vector is given $\hat{x}_{k|k-1}$ at sampling time (k) from the input u_{k-1} and state vector $\hat{x}_{k-1|k-1}$ at previous sampling time ($k-1$). The first time we go through two points of initial estimation: Point one: predefine the state measurement noises covariance matrix Q and R . Point two: Initialize the filter error covariance matrix P . After the initialization of the estimated matrix then, we have two steps must be done in this phase:

Step 1. Project the state ahead: the predicted state estimate is determined by;

$$\hat{x}_{k|k-1} = f(\hat{x}_{k-1|k-1}, u_{k-1}) \quad (23)$$

$$\text{Where } f(\hat{x}_{k-1|k-1}, u_{k-1}) = \hat{x}_{k-1|k-1} + T_s \dot{\hat{x}}_{k-1|k-1} \quad (24)$$

Step 2. Project the error covariance ahead: the predicted covariance estimate is calculated as;

$$P_{k|k-1} = F_k P_{k-1|k-1} F_k^T + Q_{k-1} \quad (25)$$

$$\text{Where } F_k = \left. \frac{\partial f(\hat{x}_{k-1|k-1}, u_{k-1})}{\partial x_{k-1}^T} \right|_{x_{k-1} = \hat{x}_{k|k-1}} ; H_k = \left. \frac{\partial h(x_k)}{\partial x_k^T} \right|_{x_k = \hat{x}_{k|k-1}}$$

4.1.2. Correction-observation phase (update)

The updated states estimate $\hat{x}_{k|k}$ which are obtained from the predicted estimated states $\hat{x}_{k|k-1}$ by adding a correction term $K_k \tilde{y}_k$ to the predicted value. So, three steps are defined:

Step 1. Compute the Kalman gain K_k : defined by the expression;

$$K_k = P_{k|k-1} H_k^T (H_k P_{k|k-1} H_k^T + R_k)^{-1} \quad (26)$$

Step 2. Update state estimation with measurement: the expression of the updated state estimate at the output of the observer is given by;

$$\hat{x}_{k|k} = \hat{x}_{k|k-1} + K_k \tilde{y}_k \quad (27)$$

$$\text{Where } \tilde{y}_k = y_{k|k} - \hat{y}_{k|k-1} \quad (28)$$

With, $y_k = h(x_k)$: actual output vector; and, $\hat{y}_{k|k-1} = h(\hat{x}_{k|k-1})$: predicted output vector. So, the final expression of the update states estimation is:

$$\hat{x}_{k|k} = \hat{x}_{k|k-1} + K_k [y_{k|k} - h(\hat{x}_{k|k-1})] \quad (29)$$

Step 3. Update error covariance is defined as:

$$P_{k|k} = (I - K_k H_k) P_{k|k-1} \quad (30)$$

4.2. PMSM rotor speed and position estimation using extended Kalman filter

The PMSM model with state and measurement noises is:

$$\begin{cases} \frac{dx}{dt} = f(x) + g \cdot u + w \\ y = h(x) + v \end{cases} \quad (31)$$

For the estimation using EKF, (31) is discretized directly using Euler approximation proposed in [25].

$$\begin{cases} x_k = f(x_{k-1}, u_{k-1}) + w_{k-1} \\ y_k = h(x_k) + v_k \end{cases} \quad (32)$$

$$\text{Moreover: } f(x_{k-1}, u_{k-1}) = \begin{bmatrix} (1 - T_S \frac{R_S}{L}) x_{1k-1} + T_S p x_{3k-1} x_{2k-1} + T_S \frac{1}{L} V_{d_{k-1}} \\ (1 - T_S \frac{R_S}{L}) x_{2k-1} - T_S p x_{3k-1} x_{1k-1} - T_S \frac{1}{L} p \Phi_f x_{3k-1} + T_S \frac{1}{L} V_{q_{k-1}} \\ (1 - T_S \frac{f}{J}) x_{3k-1} + T_S \frac{3p}{2J} \Phi_f x_{2k-1} - T_S \frac{1}{J} T_{L_{k-1}} \\ x_{4k-1} + T_S p x_{3k-1} \end{bmatrix} \quad (33)$$

$$\text{And } h(x_k) = \begin{bmatrix} x_{1k} \\ x_{2k} \end{bmatrix} \quad H_k = \begin{bmatrix} 1 & 0 & 0 & 0 & 0 \\ 0 & 1 & 0 & 0 & 0 \end{bmatrix} \quad (34)$$

$$\text{So: } F_k = \begin{bmatrix} 1 - T_S \frac{R_S}{L} & T_S p x_{3k} & T_S p x_{2k} & 0 \\ 1 - T_S \frac{R_S}{L} & 1 - T_S \frac{R_S}{L} & -T_S p x_{1k} - T_S \frac{1}{L} p \Phi_f & 0 \\ 0 & T_S \frac{3p}{2J} \Phi_f & 1 - T_S \frac{f}{J} & 1 \\ 0 & 0 & T_S p & 0 \end{bmatrix} \quad (35)$$

$$Q_k = \begin{bmatrix} 0.002 & 0 & 0 & 0 \\ 0 & 0.002 & 0 & 0 \\ 0 & 0 & 0.002 & 0 \\ 0 & 0 & 0 & 0.002 \end{bmatrix}; R_k = \begin{bmatrix} 0.02 & 0 & 0 & 0 \\ 0 & 0.02 & 0 & 0 \\ 0 & 0 & 0.02 & 0 \\ 0 & 0 & 0 & 0.02 \end{bmatrix} \quad (36)$$

5. SIMULATION RESULTS, DISCUSSION AND INTERPRETATION

The simulation results are carried out and performed in Matlab-Simulink to validate and verify the effectiveness of the proposed sensor-less nonlinear controller with regards to the following tasks: possible speed change and load torque disturbance. The used bloc scheme is described in Figure 1. The nominal PMSM parameters are shown in Table 1 and the values of the gains are: $k_\Omega = 700$; $k_d = 10000$; $k_q = 10000$.

Table 1. The PMS motor parameters

Stator resistor	$R_s = 1.4 \Omega$
d and q stator inductances	$L_d = L_q = L = 0.0058 \text{ H}$
PMSM pole pairs number	$p = 3$
Permanent flux	$\Phi_f = 0.1546 \text{ Wb}$
Inertia	$J = 0.00176 \text{ kg. m}^2$
Friction	$f = 0.000388 \text{ N. m}$
Vdc	400 volts

The used speed profile reference is shown in Figure 3 which contains four intervals:

- During the first-time interval [from 0 s to 1.5 s], The set speed changes linearly with time, until it matches a low constant value of 50 rad/second. In this case we notice that: the back-stepping controller arrives to track the evolution of the reference speed even when the load torque is introduced and the introduced EKF permits the estimated rotor speed to track the actual motor speed, presented in Figures 3 and 4.

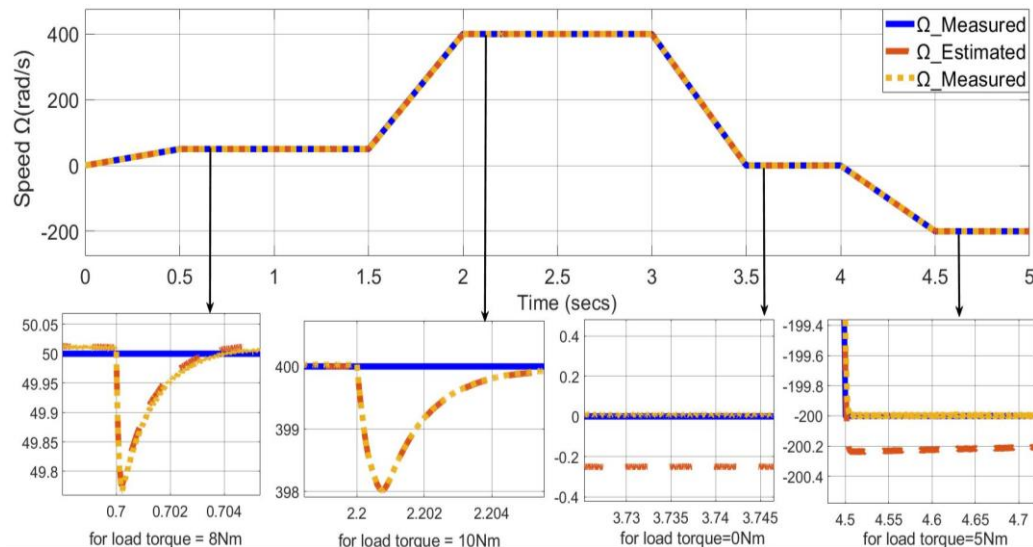


Figure 3. Dynamic speed trajectory tracking

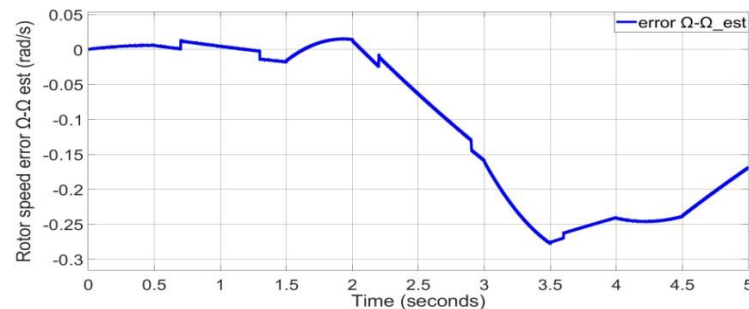


Figure 4. The speed tracking error between reel rotation speed and rotation speed estimated

- During the second time window [2 s to 3 s], the proposed controller-observer based strategy in high speed is tested where the set motor speed is kept at 400 rad/s. Figure 3, shows clearly the reliability of the used strategy as well as its strength and rigidity in all conditions, both for load torque rejection speed regulation. The controller arrives to reject the effect the load torque changing (see Figure 3) in a very short period of no more than 0.006 seconds, representing the response time. Also, in the steady state, the difference between the set and the actual speed does not exceed 2 rad/sec, which represents 0.49%. This is in fact enough to say that this strategy is consistent and robust.
- To test of the proposed strategy in severe condition and exactly during the third time interval [from 3.5 s to 4 s], a zero-set speed is chosen. As can be remarked, both the back-stepping controller continues to track properly the reference velocity, with no notable tracking error. Furthermore, the estimator continues to play the role properly, where the estimated speed matches the measured velocity adequately. This means, that the EKF can be used in all the range of the chosen reference speed profile.
- Finally, during the last interval [4.5 s to 5 s], a reverse speed operation is planned. As can be seen, notable performances are obtained, where the estimated velocity matches very well the set speed changing in both dynamic and steady state.

Figure 5, illustrates the actual and the estimated rotor position results for the PMSM drive. The error between the actual and estimated position of the rotor is due to the use of voltages and currents instead of reference voltages and currents. Through the graph Figure 6, representing the three-phase current we find that there are two observations, first a direct proportional for current amplitude. In the sense that whenever the torque changes, there is a change rapidly as load torque varies. The second concerns the rotation velocity and the current frequency is inversely proportional. For the observation mentioned above, it is accurately explained by the two curves of the current axis q and torque as shown in the two Figure 7 and Figure 8.

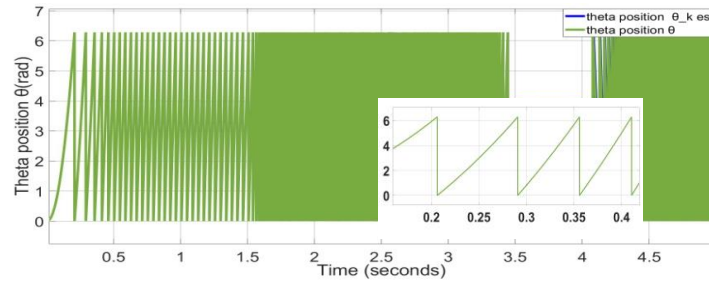


Figure 5. Dynamic position trajectory tracking

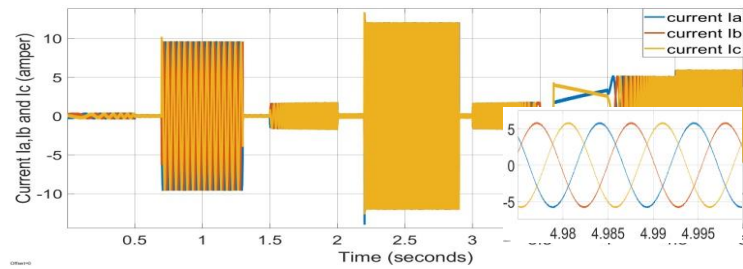


Figure 6. Three-phases Ia, Ib and Ic (A) stator current axes tracking

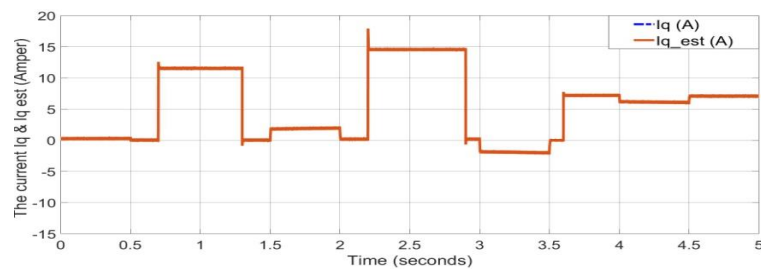


Figure 7. The iq-axis stator current

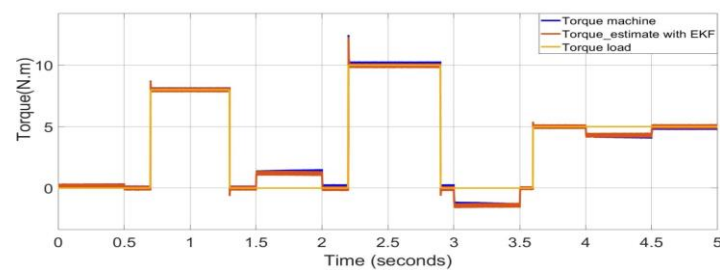


Figure 8. The torque tracking

In the present scenario, the load torque is applied from 0.7 s to 1.3 s and between [2.2 s - 2.9 s], with a magnitude of 12 Nm and 15 Nm. The Figure 3 shows very well the efficiency of the estimator. Although in the presence of external perturbation, the EKF tracks the actual value of the speed with a very small estimated error as shown on Figure 4 with the measured value of rotation speed. The estimated rotor speed follows the measured one during all changes in speed profile. According to Figure 9, the effectiveness of the proposed nonlinear controller is proved for tracking a reference speed. The i_d current is forced to zero, which matches with the vector control technique idea, and Figure 9 illustrates that.

In Figure 10, we notice that this error graph evolution over the time between the measured current (I_{d_mes}) and the estimated (I_{d_est}) is very small does not exceed the range $[-2 \times 10^{-5}, 2 \times 10^{-5}]$ it is almost

equal to the zero value. Now this proves that, the estimation algorithm the FKE is very reliable and robust concerning the parameters of the system such as the load torque or others. Figure 10 shows the measured electromagnetic torque evolution over the time span. As can be seen, the motor torque tracks adequately the evolution of the load torque, with adequate sign, concerning the speed direction operation. The locus of the stator flux Φ_α - Φ_β is shown in Figure 11. It can be seen, that in the stator reference frame, the curve is elliptic, with no chattering phenomenon remarks, which proves that the both stators flux Φ_α - Φ_β are sinusoidal.

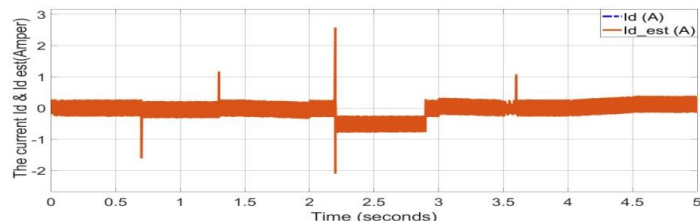


Figure 9. The Id and Id_est -axis stator current tracking

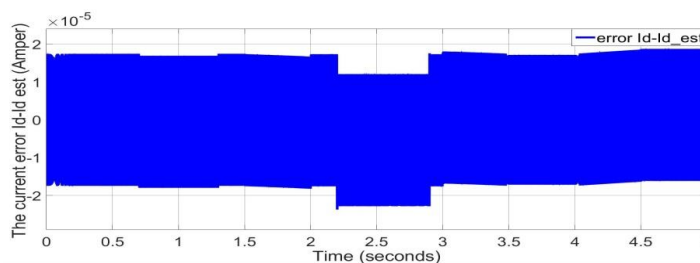


Figure 10. The current tracking error between Id and Id_est (A)

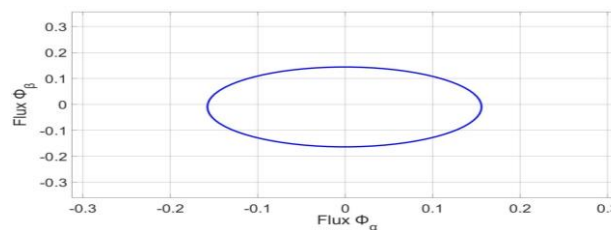


Figure 11. The locus of the stator flux Φ_α - Φ_β

5.1. Test of the robustness of sensorless control with echelon profile of speed

Figures 12 and 13 show the PMSM speed responses while expediting up the rotor speed from 0 to 300 rad/s and decreasing up of rotor speed at stopping then changing the rotor direction to -200. The reference speed is changed in a period of 1 s with a sequence [50 rad/s], [100 rad/s], [200 rad/s], [300 rad/s], and [-200 rad/s]. Figure 12 indicates that the optimal EKF estimated rotor speed is closely tracked against the reference speed and overlaps the rotor speed sensor. As the rotor speed increases, the external load becomes higher. Therefore, more torque is needed in the engine. The current id is almost zero and has a few small pulses when shifting gears. Figure 13 is more clarified with the zoom option at each step.

Table 2 and Figure 13 illustrate the performance of the system when changing the disturbance of the external load and the reference speed. When the machine is started increasing the rotor speed in the sequence of [50 rad/s], [100 rad/s], [200 rad/s], [300 rad/s], and [-200 rad/s]. The rotor speed reaches 300 rad/s after 3 s (nominal speed). At the instant $t=1.25$ s we apply an external load of value 5 N.m, the speed of the rotor will drop to 99.8 rad/s and stabilize again at the setpoint of 100 rad/s at the instant $t=1.252$ s. Then the speed reduction or the overshoot equals 0.2 rad/s and the recovery time equals 0.002 s.

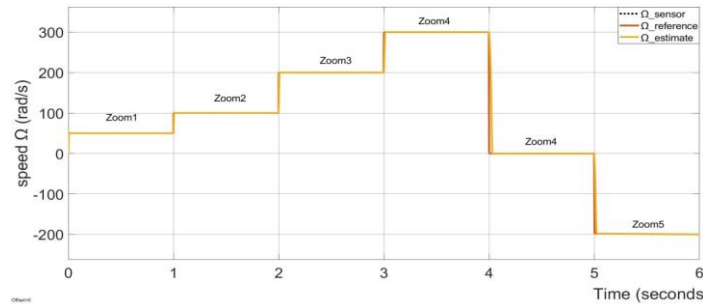


Figure 12. Dynamic speed trajectory tracking robustness

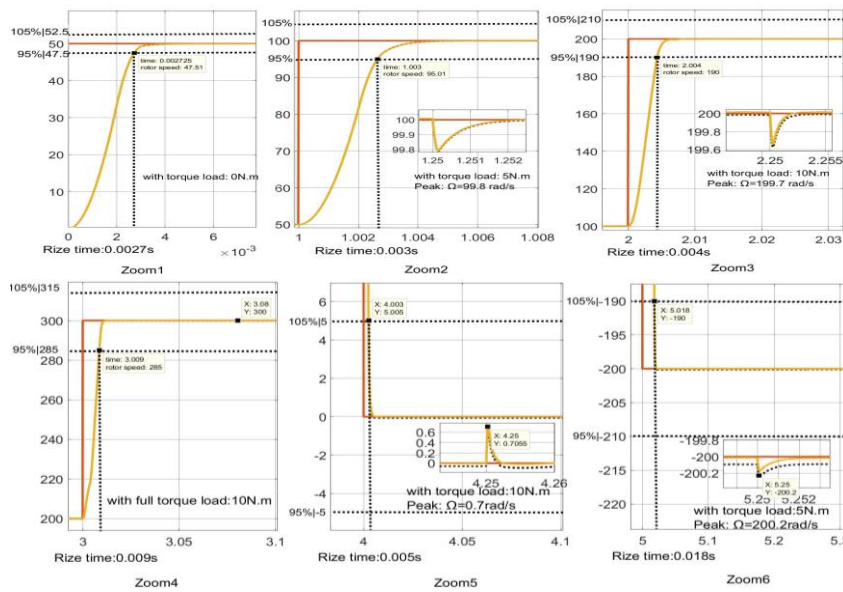


Figure 13. Zoom speed trajectory tracking robustness

The engine speed is reduced to 299.6 rad/s at time $t=2.25$ s and stabilizes again at the value 200 rad/s at time $t=2.252$ s when the load torque is increased to 10 Nm. The decreasing value or the overshoot equals 0.004 rad/s and the recovery time is 0.002 s. Even the electromechanical torque also is well following the load torque as shown in Figure 14 with small overshoots. We conclude from the obtained results that the operation of the engine is always running in a stable manner with this approach sensorless backstepping control algorithm using EKF estimator under dynamic load conditions. Table 3 represents the nomenclature of the used parameters in mathematical formulas.

Table 2. Performances of the controller and of sensorless EKF

Time windows	Step	Performance controller parameters			Performances sensorless EKF		Parameters of controller		
		Settling time (s)	Maximum overshoot Mp While applying disturbing torque	Steady state speed (rad/s)	Steady state error ($\Omega_{mes} - \Omega_{est}$)	Steady state error ($T_{mes} - T_{est}$)	k_{Ω}	k_d	k_d
[0-1]	No load	0.0027	0%	49.995	0.02%	0.025%	700	10000	10000
[1-2]	Full load to 5 N.m	0.003	0.2%	99.98	0.03%	0.025%	700	10000	10000
[2-3]	Increased load to 10 N.m	0.004	0.15%	199.96	0.03%	0.025%	700	10000	10000
[3-4]	Full load with 10 N.m	0.009	0%	299.9	0.0375%	0.025%	700	10000	10000
[4-5]	Decreased load to 0 N.m	0.005	0.07%	0.02	0.01%	0.025%	700	10000	10000
[5-6]	Full load with 5 N.m	0.018	0.1%	-200.02	0.02%	0.025%	700	10000	10000

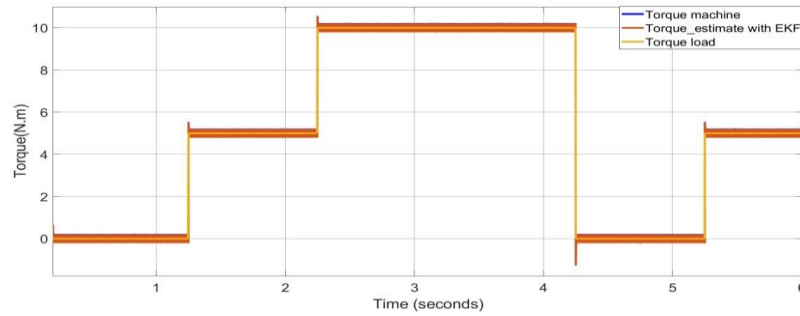


Figure 14. The torque tracking

Table 3. The nomenclature

B	Control matrix	k_{Ω} , k_d and k_q	Speed, i_d and i_q current controller PI gains
A	System state matrix	$e_{x_1}, e_{x_2}, e_{x_3}$	i_d, i_q current, and speed error
C	Output matrix	x_k	The vector state
w	External disturbance vector	P	covariance matrix State
θ	Rotor position	Q	covariance matrix noise system
Ω	Rotor angular velocity	R	Covariance matrix noise measurement
d, q	Two-axes synchronous frame quantities	T_s	Sampling period
i_q, i_d, V_d, V_q	d-q axis current and voltage components	k	Sampling index
T_L	Load torque np Number of pole pairs	0, K	Initial value and Kalman filter gain matrix
i_{qref}, i_{dref}	d-q axis reference currents	$k k - 1$	Predicted estimate

6. CONCLUSION




In this paper, the nonlinear back-stepping control strategy with EKF based on a recursive method to estimate the rotor speed position of the considered machine and to minimize the mean squared error is developed. The proposed control approach shows the dynamic speed behavior estimation taking account the parameters variation and load perturbation. The performance of the proposed controller has been investigated in numerical simulations using MATLAB environment and the presented technique shows a better dynamic speed response over the set changing speed, where the introduced controller arrives to reject the effect of the load torque in a finite time and the developed speed sensorless was successfully designed with the used EKF observer. The obtained results show that, the stochastic estimator arrives to synthesize the rotor speed in all conditions with small estimation error. In the future studies, it is planned to design an electronic interface where more parameters can be added and changed. Also, similar numerous developments can be done by using embedded system. It is also planned to try the training phase of the developed algorithm on more power systems and experimental part with the introduction of the advanced control and optimization techniques.

REFERENCES




- [1] W. Wang, X. Chen, and J. Wang, "Motor/Generator Applications in Electrified Vehicle Chassis—A Survey," in *IEEE Transactions on Transportation Electrification*, vol. 5, no. 3, pp. 584-601, Sept. 2019, doi: 10.1109/TTE.2019.2934340.
- [2] C. Venugopal, "Design of field oriented control using improved flux controller for permanent magnet synchronous motor in traction drive," *Journal of Engineering Science and Technology*, vol. 13, No. 2, pp. 524 – 539, February 2018.
- [3] J. W. Finch and D. Giaouris, "Controlled AC Electrical Drives," in *IEEE Transactions on Industrial Electronics*, vol. 55, no. 2, pp. 481-491, Feb. 2008, doi: 10.1109/TIE.2007.911209.
- [4] R. G. Shrivastava, M. B. Diagavane, and S. R. Vaishnav, "Literature Review of Permanent Magnet AC Motors and Drive for Automotive Application," *Bulletin of Electrical Engineering and Informatics*, vol. 1, no. 1, pp. 7-14, March 2012.
- [5] L. Ye and X. P. Yan, "The perspective and status of PMSM electrical servo system," *Micromotors Servo Technique*, vol. 4, pp. 30-33, 2001.
- [6] M. Lu, Y. Wang, Y. Hu, L. Liu, and Nuo Su, "Composite controller design for PMSM direct drive SGCMG gimbal servo system," *2017 IEEE International Conference on Advanced Intelligent Mechatronics (AIM)*, 2017, pp. 106-112, doi: 10.1109/AIM.2017.8014003.
- [7] J. Z. Yang, Y. X. Li, and S. Tong, "Adaptive NN finite-time tracking control for PMSM with full state constraints," *Neurocomputing*, vol. 443, pp. 213-221, July 2021, doi: 10.1016/j.neucom.2021.02.038.
- [8] R. Krishnan, "Electric motor drives: modeling, analysis and control," *Prentice-Hall New Jersey*, 2001.
- [9] K. Jezernik and M. Rodic, "High Precision Motion Control of Servo Drives," *IEEE Transactions on Industrial Electronics*, vol. 56, no. 10, pp. 3810-3816, Oct. 2009, doi: 10.1109/TIE.2009.2020709.
- [10] A. K. Singh and O. P. Roy, "Performance analysis of a PMSM drive using PID controllers," *Electronics Information and Planning*, vol. 37, no. 3, pp. 80-87, December 2010.

- [11] L. Wang, K. Xiao, L. D. Lillo, L. Empringham, and P. Wheeler, "PI controller relay auto-tuning using delay and phase margin in PMSM drives," *Chinese Journal of Aeronautics*, vol. 27, no. 6, pp. 1527-1537, Dec. 2014, doi: 10.1016/j.cja.2014.10.019.
- [12] S. Rebouh, A. Kaddouri, R. Abdessemed, and A. Haddoun, "Nonlinear Control by Input-Output Linearization Scheme for EV Permanent Magnet Synchronous Motor," *2007 IEEE Vehicle Power and Propulsion Conference*, 2007, pp. 185-190, doi: 10.1109/VPPC.2007.4544122.
- [13] R. Errouissi, M. Ouhrouch, W. Chen and, A. M. Trzynadlowski, "Robust Cascaded Nonlinear Predictive Control of a Permanent Magnet Synchronous Motor With Antiwindup Compensator," *IEEE Transactions on Industrial Electronics*, vol. 59, no. 8, pp. 3078-3088, Aug. 2012, doi: 10.1109/TIE.2011.2167109.
- [14] M. L. Corradini, G. Ippoliti, S. Longhi, and G. Orlando, "A Quasi-Sliding Mode Approach for Robust Control and Speed Estimation of PM Synchronous Motors," *IEEE Transactions on Industrial Electronics*, vol. 59, no. 2, pp. 1096-1104, Feb. 2012, doi: 10.1109/TIE.2011.2158035.
- [15] M. A. Hamida, A. Glumineau, J. de Leon, and L. Loron, "Robust adaptive high order sliding-mode optimum controller for sensorless interior permanent magnet synchronous motors," *Mathematics and Computer in Simulation*, vol. 105, pp. 79-104, November 2014, doi: 10.1016/j.matcom.2014.05.006.
- [16] J. Lau, "Adaptive backstepping based nonlinear control of interior permanent magnet synchronous motor drive," *Master thesis Lakehead University Thunder Bay Ontario*, 2005.
- [17] H. Jianhui, X. Yongxiang, and Z. Jibin, "Design and Implementation of Adaptive Backstepping Speed Control for Permanent Magnet Synchronous Motor," *2006 6th World Congress on Intelligent Control and Automation*, 2006, pp. 2011-2015, doi: 10.1109/WCICA.2006.1712710.
- [18] R. Trabelsi, A. Khedher, M. F. Mimouni, and F. M'sahli, "Backstepping control for an induction motor using an adaptive sliding rotor-flux observer," *Electric Power Systems Research*, vol. 93, pp. 1-15, December 2012, doi: 10.1016/j.epsr.2012.06.004.
- [19] Y. Kung and M. Tsai, "FPGA-Based Speed Control IC for PMSM Drive with Adaptive Fuzzy Control," in *IEEE Transactions on Power Electronics*, vol. 22, no. 6, pp. 2476-2486, Nov. 2007, doi: 10.1109/TPEL.2007.909185.
- [20] M. F. Rahman, M. E. Haque, L. Tang, and L. Zhong, "Problems associated with the direct torque control of an interior permanent-magnet synchronous motor drive and their remedies," *IEEE Transactions on Industrial Electronics*, vol. 51, no. 4, pp. 799-809, Aug. 2004, doi: 10.1109/TIE.2004.831728.
- [21] B. Singh, "Performance Evaluation of Direct Torque Control with Permanent Magnet Synchronous Motor," *Bulletin of Electrical Engineering and Informatics*, vol. 1, no. 2, pp. 165-178, June 2012, doi: 10.11591/eei.v1i2.242.
- [22] H. Muazzam, M. K. Ishak, and A. Hanif, "Compensating the performance of permanent magnet synchronous machines for fully electric vehicle using LPV control," *Bulletin of Electrical Engineering and Informatics*, vol. 10, no. 4, pp. 1923-1929, 2021, doi: 10.11591/eei.v10i4.2946.
- [23] L. Dongliang, Z. Xiehui, and C. Lili, "Backstepping control of speed sensorless permanent magnet synchronous motor," *Transactions of China Electrotechnical Society*, vol. 26, no. 9, pp. 67-72, 2011.
- [24] G. Wang, H. Zhan, G. Zhang, X. Gui, and D. Xu, "Adaptive Compensation Method of Position Estimation Harmonic Error for EMF-Based Observer in Sensorless IPMSM Drives," in *IEEE Transactions on Power Electronics*, vol. 29, no. 6, pp. 3055-3064, June 2014, doi: 10.1109/TPEL.2013.2276613.
- [25] A. Khlaief, M. Boussak, and A. Châari, "A MRAS-based stator resistance and speed estimation for sensorless vector controlled IPMSM drive," *Electric Power Systems Research*, vol. 108, pp. 1-15, March 2014, doi: 10.1016/j.epsr.2013.09.018.
- [26] O. Aydogmus and S. Sünter, "Implementation of EKF based sensorless drive system using vector controlled PMSM fed by a matrix converter," *International Journal of Electrical Power & Energy Systems*, vol. 43, no. 1, pp. 736-743, December 2012, doi: 10.1016/j.ijepes.2012.06.062.
- [27] E. G. Shehata, "Speed sensorless torque control of an IPMSM drive with online stator resistance estimation using reduced order EKF," *International Journal of Electrical Power & Energy Systems*, vol. 47, pp. 378-386, May 2013, doi: 10.1016/j.ijepes.2012.10.068.
- [28] M. Souaihia, B. Belmadani, and R. Taleb, "A robust state of charge estimation for multiple models of lead acid battery using adaptive extended Kalman filter," *Bulletin of Electrical Engineering and Informatics*, vol. 9, no. 1, pp. 1-11, February 2020, doi: 10.11591/eei.v9i1.1486.
- [29] M. Lagraoui, A. Nejmi, H. Rayhane, and A. Taouni, "Estimation of lithium-ion battery state-of-charge using an extended kalman filter," *Bulletin of Electrical Engineering and Informatics*, vol. 10, no. 4, pp. 1759-1768, August 2021, doi: 10.11591/eei.v10i4.3082.
- [30] M. A. Kamarposhti and A. A. A. Solyman, "The estimate of amplitude and phase of harmonics in power system using the extended kalman filter," *Bulletin of Electrical Engineering and Informatics*, vol. 10, no. 4, pp. 1785-1792, August 2021, doi: 10.11591/eei.v10i4.2789.
- [31] M. Karabacak and H. I. Eskikurt, "Design, modelling and simulation of a new nonlinear and full adaptive backstepping speed tracking controller for uncertain PMSM," *Applied Mathematical Modelling*, vol. 36, no. 11, pp. 5199-5213, November 2012, doi: 10.1016/j.apm.2011.12.048.
- [32] D. Janiszewski, "Extended Kalman Filter Based Speed Sensorless PMSM Control with Load Reconstruction," *IECON 2006-32nd Annual Conference on IEEE Industrial Electronics*, 2006, pp. 1465-1468, doi: 10.1109/IECON.2006.347852.
- [33] M. A. Hamida, J. de Leon, and A. Glumineau, "Experimental sensorless control for IPMSM by using integral backstepping strategy and adaptive high gain observer," *Control Engineering Practice*, vol. 59, pp. 64-76, February 2017, doi: 10.1016/j.conengprac.2016.11.012.
- [34] M. Abdelrahem, C. M. Hackl, and R. Kennel, "Simplified model predictive current control without mechanical sensors for variable-speed wind energy conversion systems," *Electrical Engineering*, vol. 99, no. 1, pp. 367-377, 2017, doi: 10.1007/s00202-016-0433-y.
- [35] P. T. Doan, T. L. Bui, H. K. Kim, G. S. Byun, and S. B. Kim, "Rotor speed estimation based on extended Kalman filter for sensorless vector control of induction motor," *AETA2013: Recent Advances in Electrical Engineering and Related Sciences*. Springer, 2014, pp. 477-486, doi: 10.1007/978-3-642-41968-3_48.




BIOGRAPHIES OF AUTHORS

Abderrahmen Kirad    was born in Ain Defla, Algeria. He received his M.Sc. from M'hamed Bougara University of Hydrocarbon and Chemistry in 2013. His research interests include electrical engineering and embedded system control. I work as designer electrical control motor at Brandt Group. He can be contacted at email: a.kirat@univ-boumerdes.dz and abderrahmen.kirad@gmail.com.



Said Grouni    got his Engineer degree in Electrotechnics (1988), a Magister degree (1992) and a Doctorate degree in Electrical Engineering (2010), from the National Polytechnic School of Algiers (ENP)-Algeria. Currently, he is a Professor at the University M'hamed Bougara of Boumerdes (UMBB), Algeria. He is as well the head a research team of control system and fault diagnosis in the Laboratory of Applied Automatic (LAA). He has supervised more than 45 subjects of studies for master degrees in electrical engineering as well as thesis supported by Magister and PhD in Automatic control. At present, he is supervising 7 engineers preparing their Ph.Ds and 3 research projects in electrical engineering. He also is a reviewer of several established reference scientific journals. His current researches include electrical drives, process control applications, electrical machines and fault diagnosis. He can be contacted at email: said.grouni@yahoo.com.



Youcef Soufi    was born in Tebessa, Algeria. He received a B.Sc. degree and Doctorate degrees from the University of Annaba, Algeria, in 1991 and 2012 respectively. And a Magister degree in 1997 in Electrical Engineering from Tebessa University, Algeria. Currently, he is a Professor in the Department of Electrical Engineering, Faculty of Sciences and Technology, Larbi Tebessi University, Tebessa, Algeria. His research interests include electrical machines, diagnostics, wind and solar energy, power electronics and drives applied to renewable and sustainable energy. He can be contacted at email: y_soufi@yahoo.fr.